Grain Boundary Engineering for Crack Bridging: Intergranular Corrosion and Stress Corrosion Crack Path Dependencies

Grain Boundary Engineering for Crack Bridging: Intergranular Corrosion and Stress Corrosion Crack Path Dependencies

* D.L. Engelberg[1] T.J. Marrow[1] L. Babout [1] R.C. Newman[2]

[1] School of Materials, The University of Manchester, M1 7HS, United Kingdom
[2] Dept. of Chemical Engineering & Applied Chemistry, University of Toronto, M5S 3E5, Canada

Abstract: The influence of environment on the degree of susceptibility of grain boundaries, and the effect of stress on the maximum intergranular stress corrosion crack length have been investigated in a Type 304 stainless steel. Fully sensitised specimens, exposed to acidified tetrathionate ($K_2S_4O_6$) solutions, indicate a shift in the intergranular corrosion susceptibility criteria with the aggressiveness of the solution. Increasing fractions of the random grain boundary population showed immunity with a rise in pH. This behaviour may be attributed to grain boundary structure related chromium depletions, with different levels of chromium being attacked by different pH solutions. IGSCC tests of statically loaded Double-Beam-Bent specimens, exposed to tetrathionate solution, showed an effect of microstructure and stress on the maximum crack length. The results are compared with existing models for percolation-like behaviour and a new grain bridging model, which includes the effect of stress. The results support the grain bridging model and highlight the disadvantages of simplified models, which include only grain boundary statistics.

Keywords: Stainless Steel, Electron Backscatter Diffraction, Grain Boundary Susceptibility, Grain Bridging, Short Crack Length Predictions.

1 Introduction

The concept of "Grain Boundary Design and Control" [1] is an attractive tool for tailoring specific material properties, in particular the intergranular corrosion (IGC) and intergranular stress corrosion cracking (IGSCC) resistance. This approach characterises the grain boundary network as a heterogeneous entity, based on the crystallographic relations of adjacent grains. Grain boundary (GB) design is typically applied to low and medium stacking fault energy face centred cubic (FCC) materials, and also known as Grain Boundary Engineering (GBE). This is commonly achieved by thermal and thermo-mechanical processing [2-4].

Electron Backscatter Diffraction (EBSD) techniques, interfaced to a Scanning Electron Microscope (SEM), are typically employed to assess statistically significant grain orientation populations [5,6]. Crystallographic as well as spatial information about the grain orientations is recorded. This data can then be used to determine a Grain Boundary Character Distribution (GBCD), which is representative of the microstructure. The GBCD is a discrete population of grain boundary types, based on either their frequencies or relative length fractions. However, it is important to be aware which of these descriptions is applied, since both may result in numerically different grain boundary character distributions. These differences are known to be related to the predominantly longer length fractions of certain boundary types [7].

The Coincidence Site Lattice (CSL) model is most frequently used to categorise individual grain boundary characters [8]. The CSL model describes the coincidences between the misoriented point lattices of the adjacent grains, which are defined by a common rotation axis and angle. The inverse volume density of the coinciding lattice points is used to assign the grain boundary character (Σ-designation). Grain boundary intersections can then be classified according to their participating CSL grain boundary types into 0-, 1-, 2- and 3-CSL Triple Junctions (TJ) [9], where CSL may refer to twin boundaries (Σ3) or higher Σ values, depending on the important properties of the boundaries [9,10].

For example, low CSL GB's up to Σ29 are often considered to be resistant against intergranular degradation processes, such as intergranular corrosion [3], intergranular stress corrosion cracking [11] or intergranular embrittlement [12]. However, investigations concerning the nature of resistant entities show a broad range of GB immunity criteria reported for such phenomena. For instance, (i) exclusion of "neutral" twins from the resistant low CSL GB population (≤Σ29) [13], (ii) inclusion only of twins (Σ3) as resistant [10], (iii) considering only the coherent twin GB population to be resistant [14], or (iv) considering only GB's with $\Sigma = 8n + 3$ ($n \geq 0$) as resistant [15]. The deviation from the exact CSL misorientation (Δθ [16,17]) is also known to be important. Increased deviation of boundaries from the exact CSL misorientation has been observed to give increased susceptibility to intergranular corrosion [17] and also an increased degree of sensitisation in austenitic stainless steels [18]. The CSL description also does not describe the orientation of the grain boundary plane, which can be important [19]. Additional factors which can also influence the behaviour of the microstructure include (i) the sensitisation parameters (e.g. time / temperature), (ii) the nature of the degradation mechanism (e.g. corrosion of a Cr-depleted zone, dissolution of Cr-Carbides and embrittlement due to segregated elements), (iii) the clustering of certain GB types [20] and (iv) the role of resistant features which may retard, divert or arrest the intergranular degradation process. Many factors are therefore involved in intergranular degradation phenomena.

This paper addresses the relationship between the environment and the selective susceptibility of the grain boundaries in a sensitised Type 304 stainless steel. The role of resistant boundaries in retarding and arresting an advancing intergranular stress corrosion crack is also considered, with the aim of predicting a likely maximum crack length, using a grain bridging model .

2 Experimental Procedure

Thermo-mechanical Processing: A Type 304 austenitic stainless steel was used (Table 1). The as received material was mill annealed (solution annealed at 1050°C and quenched with forced air). Small IGC coupon specimens with dimensions of approximately 10 mm x 10 mm x 13 mm (LxWxT) and rectangular bars of 200 mm x 20 mm x 13 mm (LxWxT) were prepared, with L parallel to the rolling direction and T perpendicular to the rolling plane of the as received plate. The bars were thermo-mechanically processed with cold rolling and subsequent heat treatment, and then sensitised, according to Table 2. Small samples for EBSD were then cut from the specimens for examination of the plane perpendicular to the rolling direction.

Table 1: Chemical composition of the Type 304 plate (wt.%).

Type	Shape	Fe	Cr	Ni	C	Mn	P	S	Si	N
Type 304	Plate	Bal.	18.15	8.60	0.055	1.38	0.032	0.005	0.45	0.038

Table 2: Processing history of IGSCC samples (Ar = Argon atmosphere / wq = water quench).

Sample	Treatment	Sensitisation
As received	-	24 hrs @ 650°C (Ar + wq)
30%/900/30	30% reduction + 900°C for 30 min. (Ar + wq)	24 hrs @ 650°C (Ar + wq)
30%/1050/10	30% reduction + 1050°C for 10 min. (Ar + wq)	24 hrs @ 650°C (Ar + wq)

IGC of As-Received Material: Coupon specimens were sensitised for 12 hrs at 650°C in argon atmosphere, followed by a water quench. All samples were ground and polished (1μm diamond paste). Analysis, using ASTM A262-practice A in conjunction with a MLI (Mean Linear Intercept) method [21], confirmed a fully sensitised microstructure. The intergranular corrosion test used an electrolyte of 0.1 M potassium tetrathionate ($K_2S_4O_6$) solution, acidified with diluted H_2SO_4 to pH 1.5, 2, 2.5 and 3, with an exposure time of 36 hrs. Post exposure, all samples were soaked in water and cleaned in ethanol. The GB's were examined in each sample and designated as (a) susceptible (the complete boundary length continuously attacked e.g. grooved), (b) semi-susceptible (the boundary non-continuously attacked or pitted) and (c) immune (no attack). EBSD was used to identify the characterised grain boundaries. Between 500 and 1000 boundaries were analysed in each sample.

IGSCC Tests: Double-Beam-Bent specimens (DBB) with dimensions of 200 mm x 20 mm x 1.5 mm were manufactured from the fully sensitised thermo-mechanical processed (TMP) bars, and loaded to 100 and 200 MPa according to ASTM G-39. The test solution consisted of 0.1 M potassium tetrathionate ($K_2S_4O_6$), acidified with diluted H_2SO_4 to pH 2.5. The exposure time was 144 hrs. After exposure, the specimens were strained in tension to 6%, to open any cracks. The samples were metallographically sectioned and the crack population assessed using extreme value statistics [22,23].

EBSD assessment: An HKL-EBSD system[1] , interfaced to a Philips XL-30 FEG-SEM was used. Three to five analysis grids along the middle fibre of the TMP specimens, each comprising an area of at least 500 μm x 500 μm and up to 750 μm x 750 μm, were examined. The IGC samples comprised areas between 100 μm x 100 μm and 300 μm x 300 μm. Step sizes of 1 μm and 5 μm were used for the GB-susceptibility and GBCD/TJD analyses respectively. An in-house developed software package (Vmap[2]) was used to extract grain orientation information, using the Coincidence Site Lattice (CSL) model. Brandon's criterion ($\Delta\theta=15x\Sigma^{-1/2}$) [16] was applied and low CSL GB's designated up to Σ29, including low angle grain boundaries (LAGB or Σ1). The LAGB were defined within the misorientation range of 1.6° to 15°. Grain sizes were determined, both including and excluding the Σ3 twin boundaries. Averaged mean values of at least 3 measurements were then used to describe the GBCD and TJD, in terms of frequency (e.g. number of occurrences). Uncertainties were reported as the measurement standard deviation range about the mean.

3 Results and Discussion

3.1 Grain Boundary Susceptibility

The influence of solution pH on IGC is shown in Figure 1. The low pH-solutions (pH 1.5 – 2) show heavily corroded grain boundary networks, with very significant grain dropping at pH 1.5. This is consistent with weight loss observations [2]. Decreasing susceptibility was observed with increasing pH, with clusters of attacked boundaries. At pH 3, the sample showed only very little and spatially isolated attack.

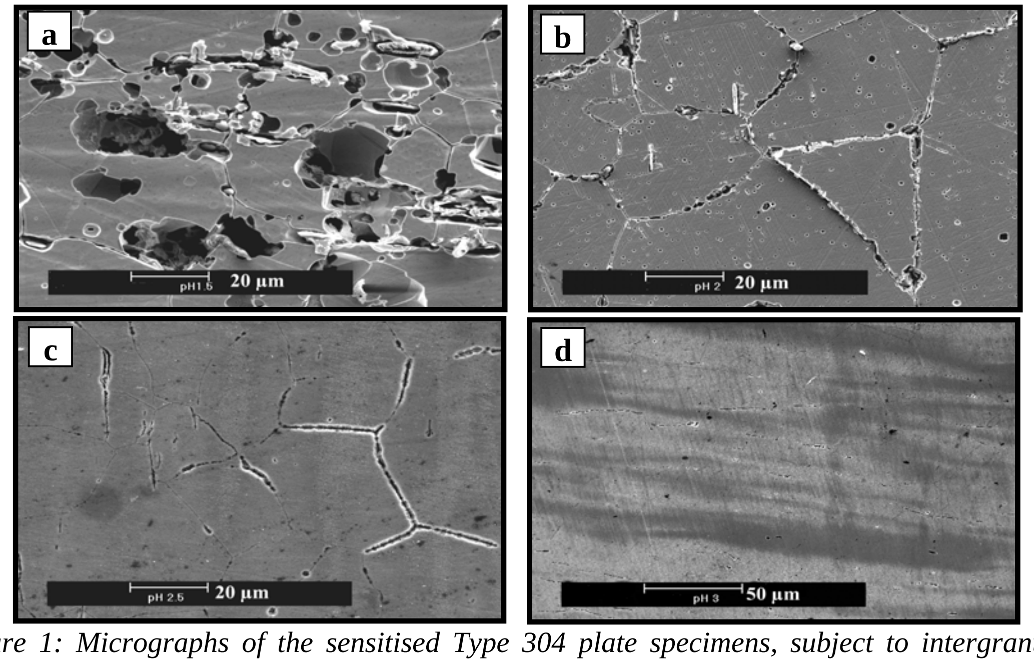

Figure 1: Micrographs of the sensitised Type 304 plate specimens, subject to intergranular corrosion tests in a $K_2S_4O_6$ solution, with (a) pH 1.5, (b) pH 2, (c) pH 2.5 and (d) pH 3.

The assessed grain boundary populations at pH 2 and pH 2.5 are given in Figure 2, as the fraction of immune, semi-susceptible and susceptible (corrosion) grain boundaries. The pH 1.5 sample was not analysed due to excessive grain dropping, and the pH 3 sample had an

---

[1] HKL Technology A/S, http://.www.hkltechnology.com

[2] Vmap, http://www.umist.ac.uk/material/staff/academic/fjh/Vmap.htm

insufficient number of attacked grain boundaries. The susceptibility of the low-CSL boundaries (≤Σ29), including LAGB and twins (Σ3) were apparently unaffected by pH. In each case, the number of twin and random boundaries analysed were around 35% to 50% of the total population, whereas the LAGB and low CSL (5-29) were around 5 to 10%. Consequently, the trends observed for the twin and random boundaries are statistically significant.

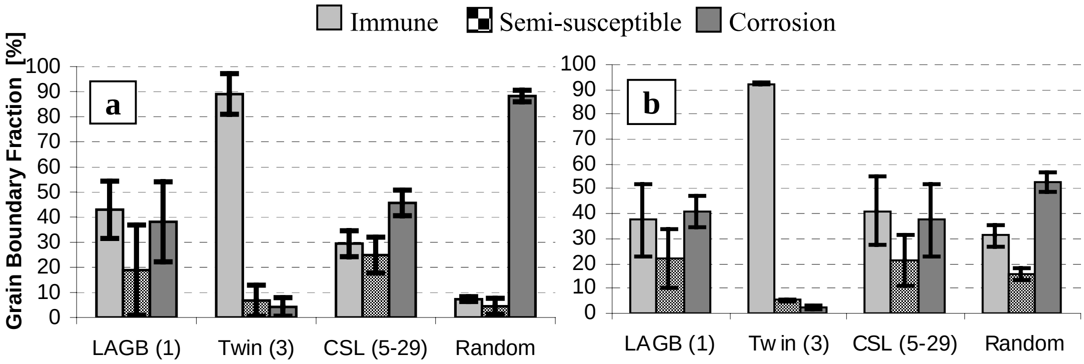

Figure 2: Immune, semi-susceptible and susceptible (corrosion) GB fractions of samples exposed unstressed to $K_2S_4O_6$ solutions at a.) pH2 and b.) pH 2.5.

Polythionate solutions [24], and in particular the tetrathionate ion [25], are known to attack chromium depleted zones [26]. The degree of intergranular corrosion is therefore determined by the degree of chromium depletion, which is affected by the grain boundary character (CSL) and the sensitisation treatment [18,27]. For example, 1 hr sensitisation at 650°C of a Type 304 stainless steel showed less than 12% Cr at a random grain boundary, over 18% Cr at a twin (Σ3) grain boundary and approximately 15% at a Σ13b grain boundary [28]. However, increasing deviations from the exact CSL misorientation, gave also an increased propensity to sensitisation and intergranular corrosion [18]. The degree of chromium depletion at a given sensitisation treatment may therefore not fully be described by the CSL notation alone. Twin boundaries (Σ3) were generally found to be most resistant (Figure 2). Coherent twins have a very low deviation from the exact CSL misorientation (typically $\Delta\theta/\Delta\theta_{max}<0.2$ [29,30]), and hence a very low grain boundary free energy [29] with associated degree of sensitisation [18]. Incoherent twins have a higher energy state [30], and probably account for the observed attacked twins [27]. A simple description based on the grain boundary CSL character is therefore only indicative of corrosion resistance, with a boundary characterised as a higher CSL, but with a low deviation, potentially having more resistance than a boundary classified as lower CSL, but with a high degree of deviation. Such behaviour is seen, for example, in intergranular corrosion of aluminium [31] and sulphur-doped nickel [32].

The effect of pH on grain boundary susceptibility can be understood in terms of the chromium concentrations, which has been shown to be a function of the electrochemical passivation potential in Fe-Ni-Cr (10% Ni, 0-20% Cr) alloys. Grain boundaries with lower chromium contents have more positive passivation potentials, with higher chromium contents having an increased passivation propensity [33]. Potential alterations are therefore able to shift the chromium concentration susceptibility criteria, which is in parallel related to the grain boundary structure. Typical compound potential-pH diagrams of the Fe-S-H_2O system, indicate that changes in the tetrathionate solution pH, result in a shift of the redox potential [34]. A higher solution pH decreases the passivation potential and/or critical current density, which would be sufficient to deactivate grain boundaries of lower chromium concentrations, and vice versa. This would explain the observed effect of pH on the corrosion of the random grain boundaries.

The grain boundary character distribution, in terms of the CSL notation is only a partial description of the chromium depletion. The distribution of susceptible GB's in the microstructure at a constant sensitisation treatment is therefore a function of environment and the GB structure. Both must be taken into account to understand the susceptibility to intergranular corrosion. Consequently, in some environments for stainless steel only one particular grain boundary character type is immune [10], or only those of a single grain boundary character which have low deviation angles are immune [14]. A more complete understanding of intergranular corrosion of sensitised stainless steels would be obtained if data were available to relate the GB chromium concentration to the GB structure.

3.2 Intergranular Stress Corrosion Cracking

IGSCC tests at two stress levels were carried out, with three microstructures. The microstructure data are given in Table 3. The as received material shows the highest CSL and twin GB fractions. The 900/30 has the smallest grain size. The crack populations, described by the extreme value distribution, are given in Figure 3. The parameter y, which is derived from the rank of the crack size in the ordered series of n observations [22,23], describes the probability of occurrence of a crack of a given size. This provides a convenient method of describing the population of observed cracks, with comparisons in the maximum likely crack length in the test specimen being made at equivalent values of y (Table 4). The crack lengths fit the extreme value distribution well, except for the as received sample which may have a bi-modal distribution. Significant effects of microstructure and stress are observed, with the shortest cracks observed in the 900/30 microstructure. Increasing stress increased the maximum crack length, most significantly in the as-received microstructure, and caused failure of the 1050/10 microstructure within 48 hours.

Table 3: Microstructure data: Grain sizes determined by including (GS-A) and excluding twins (GS-B) and their grain boundary (F) and triple junction (n-CSL) frequencies .

Sample	GS [μm]-A	GS [μm]-B	F_{CSL} [%]	$F_{\Sigma 3}$ [%]	0-CSL [%]	1-CSL [%]	2-CSL [%]	3-CSL [%]
As received	20.63±3.1	26.5±4.5	35.2±3.2	21.8±0.7	27.8±1.7	52.4±1.0	13.8±1.1	5.9±3.1
900/30	9.51±0.2	11.4±0.3	27.2±0.8	13.3±0.2	43.0±1.0	43.8±1.0	11.6±0.8	1.6±0.3
1050/10	18.86±0.4	23.7±0.7	28.9±0.7	16.4±0.4	36.6±0.9	49.0±0.2	10.9±0.3	3.5±0.4

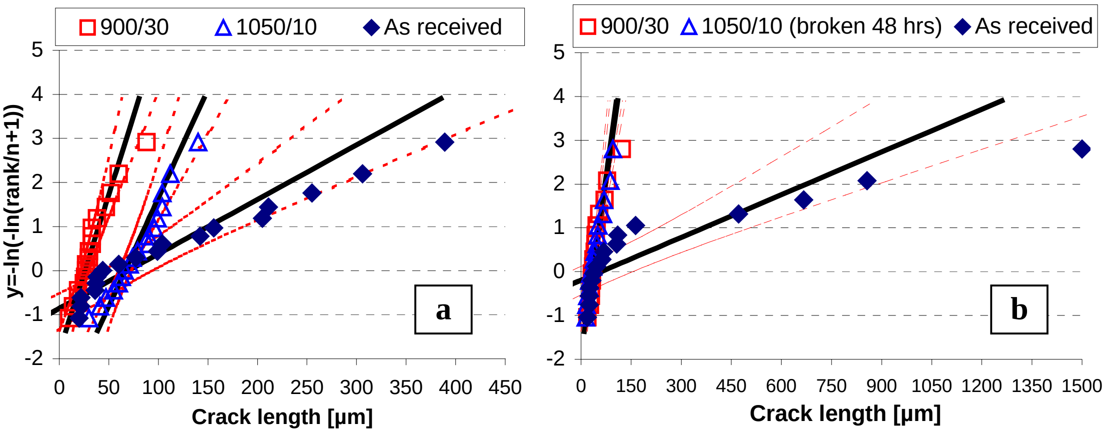

Figure 3: Crack length distributions of the IGSCC tested samples at a.) 100 MPa and b.) 200 MPa. Best fits obtained using the moments method (solid lines), with a 95% confidence interval.

Percolation-like models [10,13,35] for intergranular stress corrosion have been developed to predict that maximum likely crack length as a function of grain size and grain boundary character or triple junction distribution. The basic premise of these models is that the crack is arrested by non-favourable boundaries or triple junctions. The predicted arrest length depends on the frequency of such boundaries, and is sensitive to grain size. These models do not predict any effect of stress. Three dimensional tomography has shown that resistant grain boundaries can be by-passed by the crack, leading to crack bridging ligaments [36]. Such features have also been reported by other authors [14,19], but their influence on crack propagation has not been considered. A new model has postulated that these ligaments have a mechanical shielding effect on the crack tip, with a consequence that the maximum crack length developed in a given microstructure are sensitive to applied stress and the frequency of such bridges. The model also predicts a microstructure dependent threshold stress, above which unstable cracking occurs [37]. The model currently assumes that the frequency of bridges is determined by the number of low-CSL boundaries, which are regarded as resistant to stress corrosion cracking.

The general ranking of the microstructures observed in the IGSCC tests is consistent with both the percolation-type and bridging models, with greatest resistance in the finer grain size 900/30. However, the observation of significantly longer crack lengths at higher stress supports the bridging concept. It is likely that 200 MPa exceeds the threshold stress in the 1050/10 microstructure, and possibly also in the as-received microstructure.

The fraction of boundaries in the microstructure that are resistant to intergranular corrosion is sensitive to the environment and microstructure (Figure 2, Table 3). This indicates that crack bridging ligaments may result from both random and low-CSL boundaries. Consequently the development of crack tip shielding may also be sensitive to the test environment. The data obtained by these tests is currently being used to develop the crack bridging concept into a robust model for intergranular stress corrosion in thermo-mechanically processed microstructures.

Table 4: The effect of microstructure and stress on the maximum crack length observed (bold). Normalized length fractions (grain size without twins) are shone in brackets. The mean and 95% confidence limits of the extreme value fit to the crack population are also given for an analysed surface length of 90 mm (y=3). (failed after 48 hrs).*

Stress	As received	900 / 30	1050 / 10
100 MPa	**389 µm** (14.7) / 312±78 µm	**88 µm** (7.7) / 68±13 µm	**140 µm** (5.9) / 127±20 µm
200 MPa	**1500 µm** (failed) / 982±299 µm	**122 µm** (10.7) / 93±18 µm	**[96 µm** (4.1)]* / 86±17 µm

4 Conclusion

- The grain boundary susceptibility of sensitised 304 stainless steel, exposed to acidified tetrathionate solution, depends on the solution pH.
- The intergranular stress corrosion crack length developed in static tests is sensitive to both microstructure and applied stress.
- These observations are consistent with the predicted effects of crack tip shielding, due to the formation of crack bridging ligaments at resistant boundaries.

Acknowledgements: The authors would like to acknowledge Prof. F.J. Humphreys for the provision of his software (Vmap) and also for the financial support of Rolls-Royce Marine.

5 References

[1] T.Watanabe, *Res. Mechanica*, 1984, 47.
[2] D.Engelberg, *PhD-Thesis*, The University of Manchester, 2005.
[3] M.Shimada, H.Kokawa, Z.J.Wang, Y.S.Sato, I.Karibe, *Acta Mater.*, 2002, **50**, 2331.
[4] G.Palumbo, *US Patent 5,702,543*, 1997.
[5] B.Alexandreanu, G.S.Was, *Phil. Mag. A*, 2001, **81**, 1951.
[6] F.J.Humphreys, *Journal of Materials Science*, 2001, **36**, 3833.
[7] V.Randle, *Interface Science*, 2002, **10**, 271-277.
[8] H.Grimmer, W.Bollmann, D.H.Warrington, *Acta Cryst.*, 1974, **A30**, 197.
[9] P.Fortier, W.A.Miller, K.T.Aust, *Acta Mater.*, 1997, **45**, 3459.
[10] V.Y.Gertsman, M.Janecek, K.Tangri, *Acta Mater.*, 1996, **44**, 2869.
[11] K.T.Aust, U.Erb, G.Palumbo, *Mat. Sci. and Eng.*, 1994, **A176**, 329.
[12] U.Krupp, W.M.Kane, X.Liu, O.Dueber, C.Laird, C.J.McMahon Jr., *Mat. Sci. & Eng.*, 2002, **A349,** 213.
[13] E.M.Lehockey, A.M.Brennenstuhl, I.Thompson, *Corrosion Science*, 2004, **46**, 2383.
[14] V.Y.Gertsman, S.M.Bruemmer, *Acta Mater.*, 2001, **49**, 1589.

[15] S.Yamaura, Y.Igarashi, S.Tsurekawa, T.Watanabe, *Acta Mater* , 1999, **47**, 1163.
[16] B.G.Brandon, *Acta Metal.*, 1966, **14**, 1479.
[17] G.Palumbo, K.T.Aust, E.M.Lehockey, U.Erb, P.Lin, *Scripta Mat.*, 1998, **38**, 1685.
[18] H.Kokawa, M.Shimada, Y.S.Sato, *Journal of the Min. Met. & Mat. Soc*, 2000, **52**, 34.
[19] Y.Pan, B.L.Adams, T.Olson, N.Panayotou, *Acta Mater.*, 1996, **44**, 4685.
[20] M.Frary, C.A.Schuh, *Phys. Review*, 2004, **B69**, 134115.
[21] D.B.Wells, J.Stewart, A.W.Herbert, P.M.Scott, D.E.Williams, *Corrosion*, 1989, **45**, 649.
[22] E.J.Gumbel, *Statistics of Extremes*, Columbia University Press, 1958.
[23] M.Kokawa, *Introduction to Life Prediction of Industrial Plant Materials – Application of Extreme Value Statistical Method for Corrosion Analysis*, Allerton Press, 1994.
[24] C.H.Samans, *Corrosion*, 1964, **20**, 256t.
[25] S.Ahmad, M.L.Mehta, S.K.Karaf, I.P.Saraswat, *Corrosion*, 1982, **38**, 347.
[26] H.H.Horowitz, *Corrosion Science*, 1983, **23**, 353.
[27] B.W.Bennet, H.W.Pickering, *Metall. Trans.*, 1987, **18A**, 1117.
[28] H.Y.Bi, H.Kokawa, Z.J.Wang, M.Shimada, Y.S.Sato, *Scripta Mat.*, 2003, **49**, 219.
[29] C.B.Thomson, V.Randle, *Scripta Mat.*, 1996, **35**, 385.
[30] C.B.Thomson, V.Randle, *Acta Mater.*, 1997, **45**, 4909.
[31] S.H.Kim, U.Erb, K.T.Aust, *Scripta Mat..*, 2001, **44**, 835.
[32] G.Palumbo, K.T.Aust, *Acta Metall. Mater.*, 1990, **38**, 2343.
[33] T.M.Devine, *Corrosion Science*, 1990, **30**,135.
[34] R.C.Newman, K.Sieradzki, *Corrosion Science*, 1983, **23**, 363.
[35] G.Palumbo, P.J.King, K.T.Aust, U.Erb, P.C.Lichtenberger, *Scripta Metall. Mater.*, 1991, **25**, 1775.
[36] T.J.Marrow, L.Babout, B.J.Connoly, D.Engelberg, G.Johnson, J.-Y.Buffiere, P.J.Withers, R.C.Newman, *Proc. EICM-2*, 2004, **-in press-.**
[37] D.L.Engelberg, T.J.Marrow, R.C.Newman, L.Babout, *Proc. EICM-2*, 2004, **-in press-.**